ELSEVIER

Nuclear Physics A681 (2001) 100c–107c

NUCLEAR PHYSICS A

www.elsevier.nl/locate/npe

Chiral phase transition in high-energy collisions

Jørgen Randrup[a*]

[a]Nuclear Science Division, Lawrence Berkeley Laboratory, Berkeley, California 94720

High-energy collisions provide unprecedented opportunities for making make global explorations of chiral symmetry in strongly interacting matter. This presentation reviews the general features of the chiral phase diagram, explains the character of the non-equilibrium dynamics occurring in the collision zone and its expected effects, and illustrates suitable methods of analysis by which signals may be extracted from the experimental data.

1. INTRODUCTION

Phase transitions in strongly interacting systems provide an important focal point in modern physics. Of particular interest in the context of relativistic heavy ion research are the liquid-gas phase transition in dilute and fairly cold nuclear matter, the chromodynamic deconfinement transition expected at high pressures, and the restoration of (approximate) chiral symmetry at high temperature. The present discussion is concerned with this latter phenomenon.

Due to the relative smallness of the u and d quark masses, chiral symmetry is an approximate symmetry in the non-strange sector of the strong interaction. Moreover, in the familiar low-energy world, it is spontaneously broken and the chiral order parameter acquires a large value in vacuum, $\langle\bar{q}q\rangle = f_\pi \approx 92$ MeV. As the system is agitated, this chiral alignment will tend to weaken and, at sufficiently high temperatures, the system will approach perfect invariance with regard to chiral rotations. For a pedagogical introduction into the concepts of chiral symmetry in nuclear physics, see Ref. [1].

The advent of high-energy nuclear collisions offers an opportunity for investigating the behavior of this fundamental symmetry over a wide range of environments. We therefore first discuss the general features expected for systems in statistical equilibrium, concentrating on the simplest scenario of a baryon-free environment.

It is expected that the high-energy collisions planned at RHIC will lead to energy densities reached at mid rapidity that exceed the critical value for the restoration of chiral symmetry. If indeed the transient occurrence of such a hot region causes the local order parameter to become significantly reduced in magnitude, then its subsequent non-equilibrium relaxation towards the normal vacuum may generate large-amplitude coherent oscillations of the pion field. This novel phenomenon is commonly referred to as *disoriented chiral condensates* (DCC) and we include a discussion of its possible observational effects. For DCC reviews, see Refs. [2–4].

*Supported by the Director, Office of Energy Research, Office of High Energy and Nuclear Physics, Nuclear Physics Division of the U.S. Department of Energy, under Contract No. DE-AC03-76SF00098.

PII S0375-9474(00)00489-9

2. STATISTICAL EQUILIBRIUM

A simple theoretical tool for the global exploration of chiral symmetry in baryon-free systems is provided by the linear σ model. It describes the O(4) chiral field $\boldsymbol{\phi}(\mathbf{r},t) = (\sigma,\boldsymbol{\pi})$ by means of a simple effective quartic interaction,

$$\mathcal{L} \;=\; \tfrac{1}{2}\partial_\mu\boldsymbol{\phi}\circ\partial^\mu\boldsymbol{\phi} \;-\; \tfrac{\lambda}{4}(\boldsymbol{\phi}\circ\boldsymbol{\phi}-v^2)^2 \;+\; H\sigma \quad , \; \boldsymbol{\phi}\circ\boldsymbol{\phi} \;=\; \sigma(\mathbf{r})^2+\boldsymbol{\pi}(\mathbf{r})\cdot\boldsymbol{\pi}(\mathbf{r}) \; . \tag{1}$$

The three parameters, λ, v, and H, are usually fixed to reproduce the values of the pion decay constant f_π, the free pion mass m_π, and the mass of the schematic σ meson, m_σ.

The equation of state can be conveniently studied in a semi-classical mean-field approximation [5], in which the field operators are treated as real functions, while the initial occupancies of the individual quasiparticle modes obey quantum statistics, in analogy with the familiar nuclear Hartree treatment. It is instructive to separate the field into an order parameter, which can be regarded as a constant throughout the test volume considered, and the residual part which then represents quasi-particle agitations relative to the (false) vacuum defined by the value of the order parameter, $\boldsymbol{\phi}(\mathbf{r},t) = \underline{\boldsymbol{\phi}}(t) + \delta\boldsymbol{\phi}(\mathbf{r},t)$. At a given temperature T, and for a given value of the O(4) order parameter $\underline{\boldsymbol{\phi}}$, the quasi-particle degrees of freedom are governed by a Klein-Gordon equation. Their O(4) mass tensor is diagonal in a system aligned with $\underline{\boldsymbol{\phi}}$ and invariant under rotations around that direction. The eigenvalue along $\underline{\boldsymbol{\phi}}$ is $\mu_\parallel^2$ and the three others are $\mu_\perp^2$ (with $\mu_\parallel^2 \geq \mu_\perp^2$).

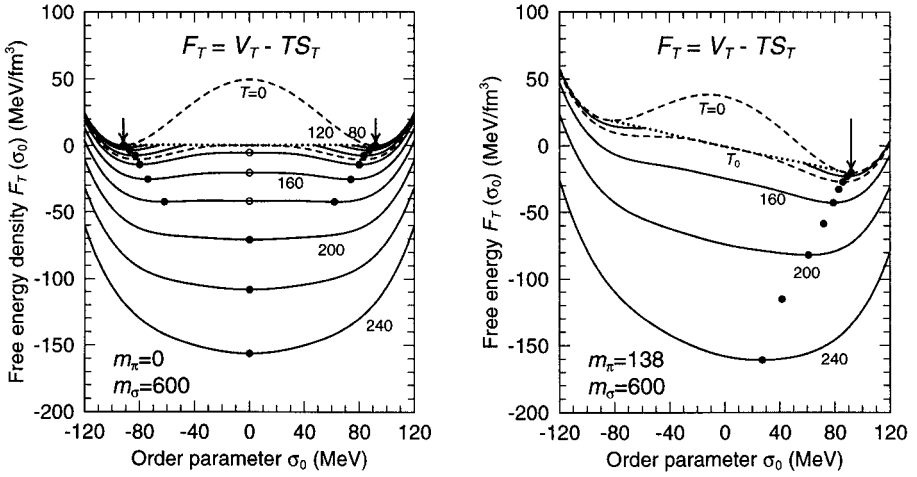

Figure 1. The free energy density F_T calculated with the semi-classical mean-field approximation to the linear σ model, as a function of the order parameter σ_0 for various values temperatures T, for either the idealized O(4) symmetric case (m_π=0) or for the physical case (m_π=138 MeV). At each T, the solid (or open) dots indicate the stable (or unstable) equilibria. For $T < T_0 = \sqrt{2}v$, the order parameter must exceed a certain minimum value before all quasiparticle modes are stable; the corresponding end points are connected by the dotted curve. The top dashed curve is the bare potential obtained for T=0.

The above separation makes it relative easy to examine the statistical properties of the system, as is best done by means of the partition function associated with the chiral field,

$$\mathcal{Z}_T = \int \mathcal{D}[\dot{\boldsymbol{\phi}}(\mathbf{r}), \boldsymbol{\phi}(\mathbf{r})]\; \mathrm{e}^{-\frac{\Omega}{T}E[\dot{\boldsymbol{\phi}}(\mathbf{r}),\boldsymbol{\phi}(\mathbf{r})]} = \int d^4\underline{\phi}\; \mathrm{e}^{-\frac{\Omega}{T}F_T(\phi_0,\chi_0)} = \int d^4\underline{\phi}\; W_T(\underline{\phi})\;. \tag{2}$$

To obtain this result, a functional integration has been made over all the quasi-particle components of the field, $(\delta\dot{\boldsymbol{\phi}}(\mathbf{r}), \delta\boldsymbol{\phi}(\mathbf{r}))$, as well as over the time-derivative of the order parameter, $\dot{\underline{\phi}}$. The relative probability for encountering a particular value of the order parameter, $\underline{\phi} = (\sigma_0, \underline{\boldsymbol{\pi}})$ is given by the usual statistical weight where the free energy density depends only on the magnitude ϕ_0 of the order parameter, and its disorientation angle χ_0 relative to the σ direction, $F_T(\phi_0, \chi_0) = V_T(\phi_0, \chi_0) + TS_T(\phi_0)$ (illustrated in fig. 1). Here V_T is the effective potential energy density for the order parameter and S_T is the entropy density carried by the quasi-particle degrees of freedom. In order to calculate these quantities it is necessary to find the self-consistent solution to the two coupled gap equations for the effective masses $\mu_{\|}$ and $\mu_{\perp}$ which depend on the magnitude of the order parameter, ϕ_0, and the thermal fluctuations of the fields, $\langle\delta\boldsymbol{\phi}_{\|}^2\rangle$ and $\langle\delta\boldsymbol{\phi}_{\perp}^2\rangle$ (which in turn depend on the masses). A solution exist when T and ϕ_0 are sufficiently large, but the lower-left part of the chiral phase diagram (see fig. 2) represents a supercritical region within which the softest pion-like modes are unstable and experience an exponential growth that is manifested in the spontaneous creation of pion pairs.

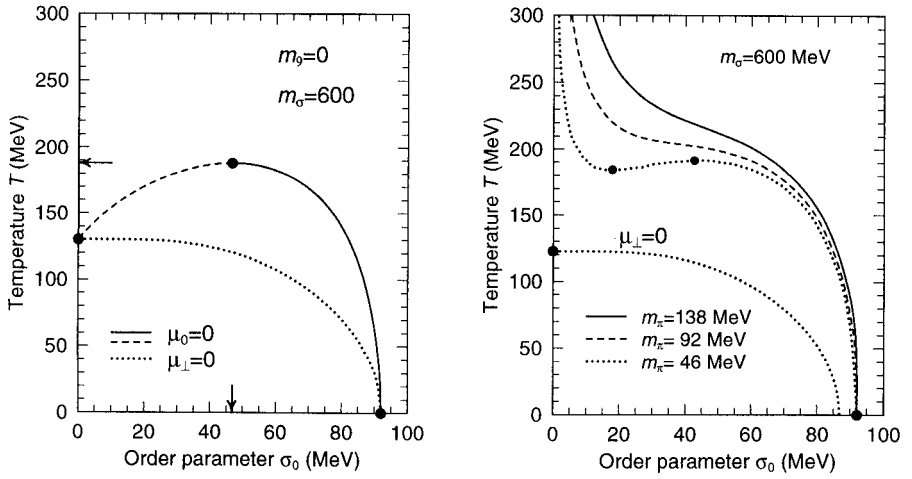

Figure 2. *Left:* The stable (solid) and unstable (dashed) equilibrium values of the order parameter $\sigma_0 = \phi_0 \cos\chi_0$ at a given quasi-particle temperature T as traced on the chiral phase diagram, for the idealized O(4) symmetric case where m_π vanishes. The dotted curve delineates the boundary defined by $\mu_\perp$=0 within which the field is supercritical. *Right:* The same quantities for three finite pion masses equal to $\frac{1}{3}m_\pi$, $\frac{2}{3}m_\pi$, and m_π (=138 MeV). The dotted curve delineates the critical boundary for the latter case.

2.1. Infinite matter

In the idealized case of perfect chiral symmetry, corresponding to a vanishing free pion mass, m_π=0, the system exhibits a first-order phase transition. Through a certain intermediate temperature range, the free energy F_T has two minima, corresponding to (meta)stable values of ϕ_0, separated by a (very shallow) maximum, at which ϕ_0 is in unstable equilibrium. Since the quasi-particle entropy increases with the order parameter, at a fixed temperature (because the effective masses grow larger), the outer minimum carries the larger statistical weight and is thus the preferred one. So the phase transition occurs at the highest T for which there are two minima. Figure 3 depicts how the effective quasi-particle masses evolve along the equilibrium path on the phase diagram. Above the transition temperature, all the masses are degenerate and grow approximately linearly.

The picture changes qualitatively when a more realistic value of m_π is employed. Adopting the actual value of 138 MeV, we find a free energy that has only a single minimum at any value of T (fig. 1) The corresponding equilibrium value of the order parameter decreases steadily as the system gets hotter and it ultimately approaches zero as T^{-2} (fig. 2). Thus the system displays a smooth crossover from the strongly broken to a weakly broken phase and perfect O(4) symmetry is never achieved. The qualitative difference is also evident in the behavior of the effective masses (fig. 3), where μ_π exhibits an initially slow but steady growth with T, while μ_σ undergoes a minimum as T moves through the crossover region, above which the masses quickly become nearly degenerate and become approximately independent of m_π (because the thermal contribution dominates).

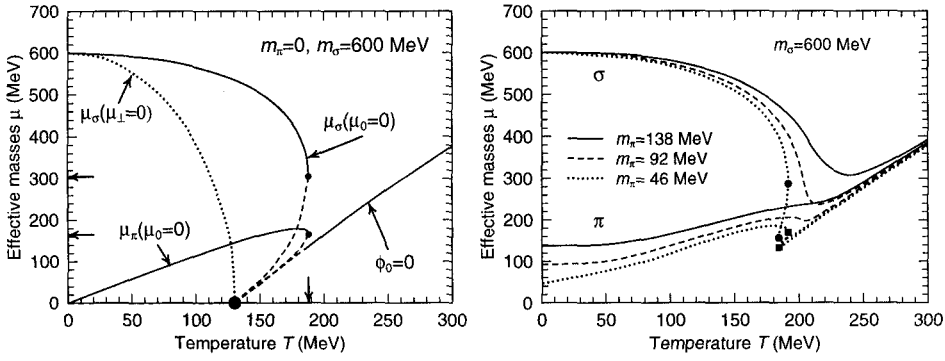

Figure 3. *Left:* The values of the effective quasi-particle masses $\mu_{||}$ and $\mu_\perp$ as functions of the temperature T, using the stable (solid) and unstable (dashed) equilibrium values of the order parameter σ_0, for the idealized O(4) symmetric case where m_π vanishes; all the masses vanish at the critical point (solid dot) and they are degenerate above the corresponding critical temperature. The dotted curve indicates the value of $\mu_{||}$ along the critical boundary where $\mu_\perp$=0. *Right:* The same quantities for the three finite pion masses considered on fig. 2 ($\frac{1}{3}m_\pi$, $\frac{2}{3}m_\pi$, and m_π). The symbols mark the inversion points.

2.2. Finite-size effects

Since the systems available for actual experimental study have a rather limited spatial extension, it is important to assess the importance of finite-size effects. Generally speaking, the statistical fluctuations in finite systems tend to wash out the sharp phase structure characteristic of infinite matter.

The importance of this effect on the temperature dependence of the order parameter is brought out in fig. 4. It is seen that the changes are most significant in the idealized O(4) symmetric scenario. In particular, it can be seen how the first-order transition obtained for m_π=0 becomes less prominent as the volume is decreased to realistic magnitudes and ultimately, for small volumes ($L\approx$5 fm), it disappears altogether. From this point on, the difference between the results obtained for the various specified values of the free pion mass is less noticeable. This finding suggests that a quantitative extraction of the matter equation of state from analysis of the small finite systems involved in actual experiments depends heavily on the availability of reliable models.

Another important finite-size effect is the fluctuation in the O(4) orientation of the order parameter $\underline{\phi}$ which is often believed to be large. However, because of the large entropy carried by the quasi-particles, even a relatively modest change in the disalignment angle χ_0 leads to a strong reduction in the statistical weight. As a result, the equilibrium distribution $P(\underline{\phi})$ remains fairly confined around the positive σ direction, as is illustrated in fig. 5. Thus, the idealized "sombrero" picture in which the order parameter has a fairly isotropic distribution at high temperatures may be somewhat misleading.

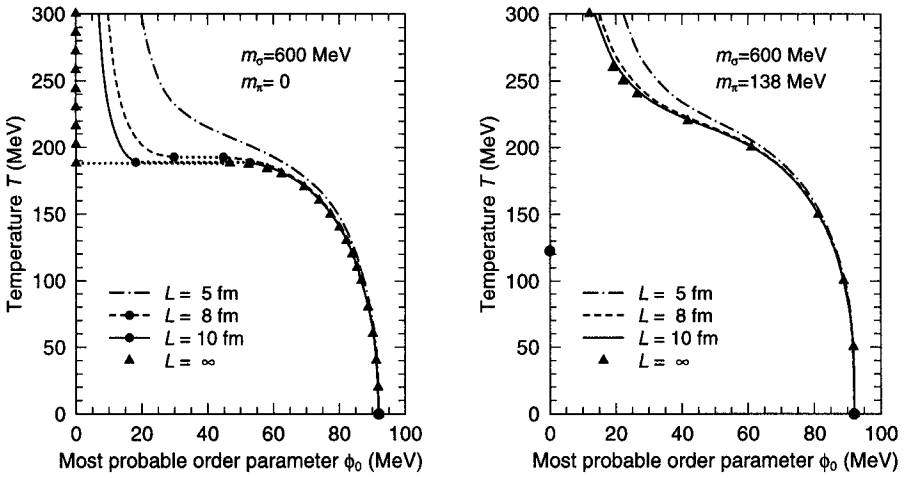

Figure 4. *Left:* The most probable values of the magnitude of order parameter, ϕ_0, as a function of the imposed quasi-particle temperature T, for m_π=0 and various values of the side length L of the cubic volume considered. The first-order phase transition obtained for $L = \infty$ remains visible for the larger volumes and is indicated by the dotted lines. *Right:* The same quantities for the physical case where m_π=138 MeV.

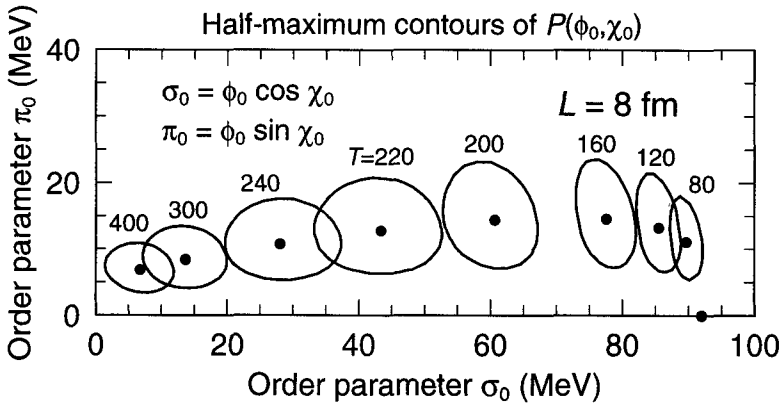

Figure 5. The *projected* equilibrium distribution of the order parameter, $P(\phi_0, \chi_0) \sim \phi_0^3 \sin^2\chi_0 W_T(\underline{\phi})$, displayed as a function of the aligned component the order parameter, $\sigma_0 = \phi_0 \cos\chi_0$, and the magnitude of its transverse component, $\pi_0 = \phi_0 \sin\chi_0$, for a cubic box of side length L=8 fm. For each temperature T, the solid dot indicates the location of the maximum in $P(\sigma_0, \chi_0)$ and the solid curve traces out the half-maximum contour, as obtained by scaling the continuum results down to the finite volume $\Omega = L^3$.

3. DYNAMICS AND OBSERVABLES

Although the idealized systems discussed above can yield very instructive insight into key features of the DCC phenomenon, it is important to consider more realistic scenarios in order to ascertain the prospects for extracting signals in actual experiments. For this purpose it is interesting to consider the evolution of a cylinder subjected to a longitudinal scaling expansion of the Bjorken type (a *Bjorken rod* [6]), since this scenario contains some of the important features expected in real collision events. In particular, it has a surface region through which the order parameter changes from its small value in the interior to its vacuum value outside and it is endowed with a rapid longitudinal expansion.

Figure 6 illustrates the phase evolution of the interior region of a Bjorken rod, as the initially hot system expands and cools while approaching a collection of free pions. It should be noted that the early evolution of the rod interior is very similar to that of the corresponding *Bjorken matter* (a very thick Bjorken rod), but later on the relaxation proceeds significantly faster due to the self-generated transverse expansion (which is absent in the matter scenario). In particular, it should be noted that the system never enters the supercritical region, so it appears that the originally envisioned quench scenario [7] may not be dynamically reachable, unfortunately. Instead, the system displays an evolution much closer to adiabatic, but with certain systematic deviations: Initially the order parameter lags behind the evolution of the effective potential, as it requires some time to start its growth, but then, once moving, it overshoots the adiabatic equilibrium value and enters into a weakly damped oscillation which quickly becomes centered around the vacuum point $(f_\pi, \mathbf{0})$. These qualitative features are rather robust with respect to changes in such features as the initial temperature and the rod radius.

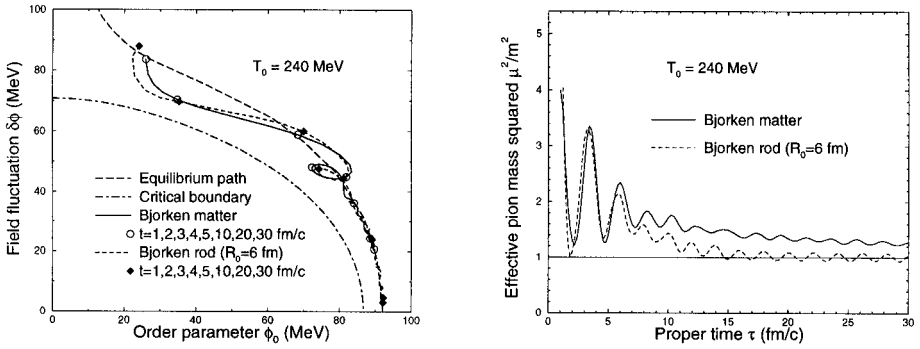

Figure 6. *Left:* Phase evolution of the interior of a Bjorken rod prepared with a bulk temperature of T_0=240 MeV and a radius of R_0=6 fm and the corresponding evolution of Bjorken matter (obtained in the limit of a very thick Bjorken rod, $R_0 \to \infty$) [6]. In order to be able to display an arbitrary non-equilibrium scenario, the average field fluctuation $\langle\delta\phi^2\rangle^{1/2} = \langle\delta\sigma^2 + \delta\pi^2\rangle^{1/2}$ has been used in place of the temperature on the vertical axis. Also shown are the equilibrium path and the boundary of the supercritical region. The rod has been probed over a hollow cylindrical volume, $1<\rho<3$ (fm). The paths are marked at successive proper times τ=1,2,3,4,5,10,20,30 fm/c. The two evolutions are similar early on, but the rod then relaxes significantly faster due to the generated transverse expansion. *Right:* The corresponding evolutions of the squared effective pion mass μ_π^2 [6].

The phase evolution is reflected in the time-dependence of the effective pion mass, as illustrated in fig. 6 (*right*): The overall decay of μ_π^2 towards the free value is overlaid with a slowly subsiding oscillation having a frequency approximately equal to m_σ. As a result, certain pion modes are being amplified [8–11].

A quantitative impression of the magnitude of this potentially observable effect can be gained from fig. 7 (*left*). The enhancement is generally confined to pions with transverse energies below 200 MeV. Taking into account that these results were obtained for rather thin rods and that the classical field treatment generally underestimates the amplification [11], one might expect perhaps as much as a 50% increase above the thermal background for the softest part of the transverse spectrum.

Moreover, since the oscillations of the order parameter are well-directed in isospace, the generated pions are correspondingly isospin polarized, a characteristic DCC feature that leads to an anomalously wide distribution of the neutral pion fraction (which, however, is hard to probe experimentally). The fact that only certain modes are selectively amplified enhances the pion multiplicity fluctuations as well, relative to the ordinary Poisson statististics. This latter effect can be brought out by considering the factorial moments of the pion multiplicity distribution, $\mathcal{M}_m = \langle N(N-1)\cdots(N-m+1)\rangle$, as illustrated in fig. 6 (*right*). It is seen that the higher factorial moments for the soft pions indeed display enhanced values, while the harder pions behave normally [6].

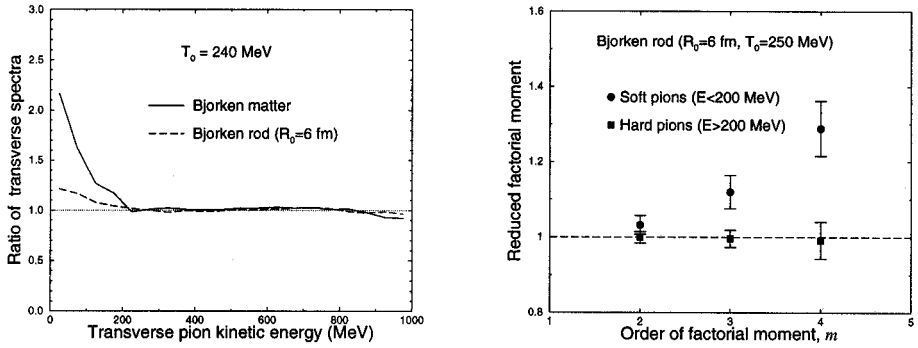

Figure 7. *Left:* The ratio between the final transverse pion spectrum, $d^3N/d^2\mathbf{p}_\perp dy$, and the associated equilibrium spectrum obtained by fitting the dynamical result with a Bose-Einstein form within the transverse energy interval 200-1000 MeV, for a longitudinally expanding rod (dashed curve) having an initial radius of R_0=6 fm and with an initial bulk temperature T_0=240 MeV, in addition to the corresponding result for $R_0 \to \infty$ [6]. *Right:* The reduced factorial moments $\mathcal{M}_m/\mathcal{M}_1^m$ obtained for a sample of rods prepared with R_0=6 fm and T_0=250 MeV and displayed as functions of the order m, for either soft (dots) or hard (squares) pions emitted within a given rapidity interval of unit length [6]. (The reduced factorial moments for a pure Poisson multiplicity distribution are all unity.)

4. CONCLUDING REMARKS

Chiral symmetry is a fundamental concept in strong-interaction physics and the exploration of the associated phase structure is an important goal in heavy-ion physics. Dynamical studies based on the linear σ model suggest the emergence of specific observable signatures with a bearing on the expected non-equilibrium relaxation of the chiral degrees of freedom induced by a high-energy nuclear collision.

REFERENCES

1. V. Koch, Int. J. Mod. Phys. E6 (1997) 203.
2. K. Rajagopal, in *Quark-Gluon Plasma 2*, Ed. R. Hwa, World Scientific (1995).
3. J.-P. Blaizot and A. Krzywicki, Acta Phys. Polon. B27 (1996) 1687.
4. J.D. Bjorken, Acta Phys. Polon. B28 (1997) 2773.
5. J. Randrup, Phys. Rev. D55 (1997) 1188; Nucl. Phys. A616 (1997) 531.
6. T.C. Petersen and J. Randrup, Phys. Rev. C61 (2000) 024906.
7. K. Rajagopal and F. Wilczek, Nucl. Phys. B404 (1993) 577.
8. D. Boyanovsky, H.J. de Vega, and R. Holman, Phys. Rev. D51 (1995) 734.
9. S. Mrowczynski and B. Müller, Phys. Lett. B363 (1995) 1.
10. Y. Kluger, V. Koch, J. Randrup, and X.N. Wang, Phys. Rev. C57 (1998) 280.
11. J. Randrup, Heavy Ion Phys. 9 (1999) 289.